

# *Z<sup>2</sup>-FET DC hysteresis: deep understanding and preliminary model*

J. Lacord<sup>1</sup>, S. Martinie<sup>1</sup>, M.-S. Parihar<sup>2</sup>, K. Lee<sup>2</sup>, M. Bawedin<sup>2</sup>, S. Cristoloveanu<sup>2</sup>, Y. Taur<sup>3</sup> and J.-Ch. Barbé<sup>1</sup>

<sup>2</sup> CNRS; IMEP-LAHC, Univ. Grenoble Alpes, Grenoble, France. <sup>3</sup>University of California University, San Diego, USA

<sup>1</sup> Univ. Grenoble Alpes, F-38000 Grenoble France  
CEA, LETI, MINATEC Campus, F-38054 Grenoble, France

E-mail: [joris.lacord@cea.fr](mailto:joris.lacord@cea.fr)

**Abstract**— *Z<sup>2</sup>-FET*, a partially gated diode, was explored for ESD application due to its sharp switching behavior [1,2]. 1T-DRAM application of *Z<sup>2</sup>-FET* has recently been evidenced [3,4] leading to an even stronger interest for this device. However, a deep explanation of physical phenomena involved in *Z<sup>2</sup>-FET* operation has not been proposed yet. In this paper, we provide a detailed description of the *Z<sup>2</sup>-FET* DC behavior based on TCAD simulations and propose corresponding analytical modeling.

**Keywords:** *Z<sup>2</sup>-FET*, 1T-DRAM, DC operation, TCAD, compact model.

## I. INTRODUCTION

*Z<sup>2</sup>-FET* (Zero Impact Ionization and Zero Subthreshold Slope FET), has first been introduced as an ESD device because of its sharp switch [1,2]. Its behavior looks like a thyristor but does not involve impact ionization for triggering. More recently, *Z<sup>2</sup>-FET* for 1T-DRAM application has been experimentally evidenced [3,4] leading to an even stronger interest for this device. Moreover, its fabrication is fully compatible with standard 28FDSOI technology [4] and does not need any additional process step. To go further and determine if *Z<sup>2</sup>-FET* could bring any benefit at application level, a compact model is needed to enable circuit design studies. However, a full explanation of physical phenomena involved in *Z<sup>2</sup>-FET* operation and compact model usable in SPICE simulator are still missing. A recent work proposed a comprehensive *Z<sup>2</sup>-FET* model describing its complete DC behavior [5]. While predictive of the I-V characteristics, its multiple implicit equations are not compact and can't be used for circuit simulation. In this paper, after describing our *Z<sup>2</sup>-FET* TCAD simulation methodology, we propose a detailed explanation of the DC behavior of *Z<sup>2</sup>-FET* based on TCAD simulations and we finally propose a full analytical model of *Z<sup>2</sup>-FET* DC operation, validated by our TCAD simulations.

## II. *Z<sup>2</sup>-FET* TCAD SIMULATION METHODOLOGY

*Z<sup>2</sup>-FET* device is a partially gated PIN diode on SOI (Fig. 1). It was experimentally demonstrated that *Z<sup>2</sup>-FET* DC operation presents sharp switching leading to a DC hysteresis [2]. This

original behavior is due to field-induced doping through top and back gates polarization which turns the device into a virtual PNP structure.

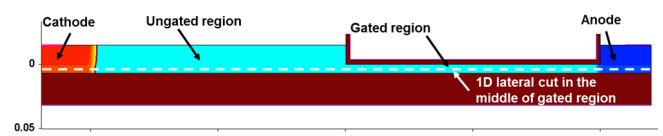


Figure 1: *Z<sup>2</sup>-FET* structure simulated with device TCAD including a representation of the 1D cut from cathode to anode used to analyse DC behavior.

We first set up a TCAD [6] methodology to evidence *Z<sup>2</sup>-FET* DC sharp switching and hysteresis. Basics physical mechanisms included in our simulations are sufficient to explore *Z<sup>2</sup>-FET* behavior, i.e. drift diffusion, constant mobility and SRH generation/recombination models. This is consistent with literature [3], which demonstrated that sharp switching phenomena in *Z<sup>2</sup>-FET* operation does not involve impact ionization. We defined basic *Z<sup>2</sup>-FET* device (Fig. 1): N-type cathode, P-type anode and intrinsic silicon body with gated and ungated lengths both equal to 200nm. We plotted anode current  $I_A$  vs anode voltage  $V_A$  for  $V_G=2V$  and  $V_B=-2V$  (values large enough to ensure sufficient field-induced doping concentration). Fig.2 shows DC hysteresis by sweeping  $V_A$  in direct (0 to 2V, dark blue line) and reverse (2 to 0V, light blue line) modes. Sharp switching in direct ( $V_A=V_{on}$ ) and in reverse ( $V_A=V_{off}$ ) bias is also captured. However, if DC TCAD *Z<sup>2</sup>-FET* is driven by current source, it leads to S-shape  $I_A-V_A$  curve (black curve of Fig.2) [1-2] exhibiting negative resistance regime, linking the two switching voltages ( $V_{on}$  &  $V_{off}$ ). We also evidence that, if  $V_G$  and/or  $V_B$  are not strong enough, *Z<sup>2</sup>-FET* behaves as a standard PIN diode (red curve, Fig.2). This behavior was expected because top and back gate need to be sufficiently polarized to build the field-induced doping PNP structure.

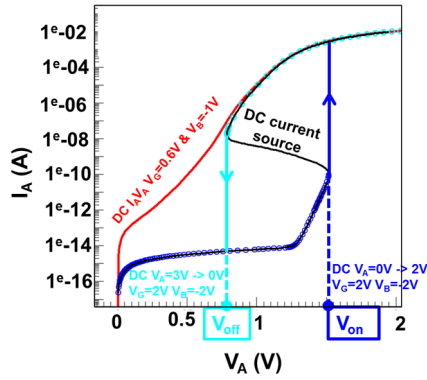


Figure 2: Comparison between  $Z^2$ -FET  $I_A$ - $V_A$  obtained by TCAD: red, dark and light blue = voltage driven; Black = current source driven.

### III. $Z^2$ -FET DC TCAD DEEP ANALYSIS

In the S-shape  $I_A$ - $V_A$  curve, five regimes can be identified for  $Z^2$ -FET DC operation (Fig.3).

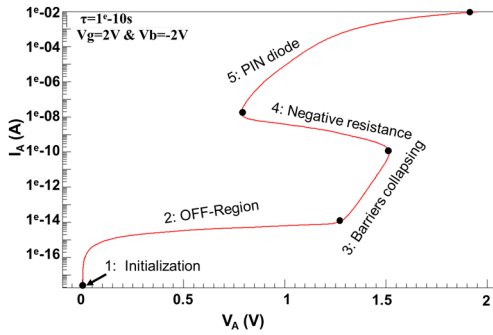


Figure 3: DC current source  $I_A$ - $V_A$  with the definition of the five DC operation regimes of  $Z^2$ -FET.

**1-Initialisation:**  $V_A=0$  and  $V_G$  and  $V_B$  are respectively positively and negatively polarized to build up N and P-type field-induced doping as illustrated in Fig.4 where carrier densities are plotted along the 1D cut pictured on Fig.1. Barrier potential is thus built up at the junction between gated and ungated regions (see Figure 5). Note that carrier density values in both gated and ungated regions correspond to inversion regime carrier densities of a MOS capacitor. The potential under the gate reaches inversion potential value of MOS capacitor, noted  $\psi_{Ginv}$ .

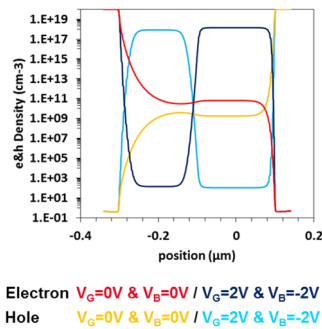


Figure 4: Carrier densities from cathode to anode during *initialization*

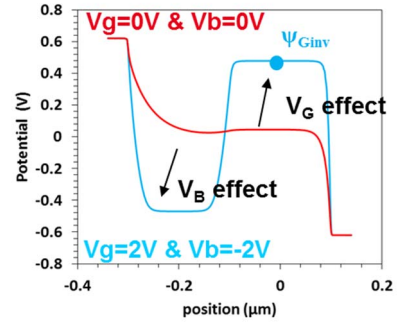


Figure 5: Potential from cathode to anode during *initialization*

For the following steps  $V_G$  and  $V_B$  are kept constant.

**2-OFF-Region:**  $V_A$  is ramped to 1.2V and  $I_A$  slightly increases. This produces a lowering of electron density under the gate (field-induced N doping is lowered, Fig.6) which reaches its minimum value, close to intrinsic carrier concentration value. This enables the PN junctions (P-anode/N-field induced body & N-cathode/P-field induced body) to stay in unpolarized state. This is confirmed by the product of electron and hole densities which everywhere is equal to the square of intrinsic carrier density ( $n \cdot p = n_i^2$ ). The lowering of electron density under the gate produces an increase of the potential, which reaches a maximum value corresponding to depletion regime in a MOS capacitor,  $\psi_{Gdep}$  (Fig.6). As potential in gated region increases and is roughly constant in ungated region, the potential barrier between gated and ungated region increases in *OFF-region*.

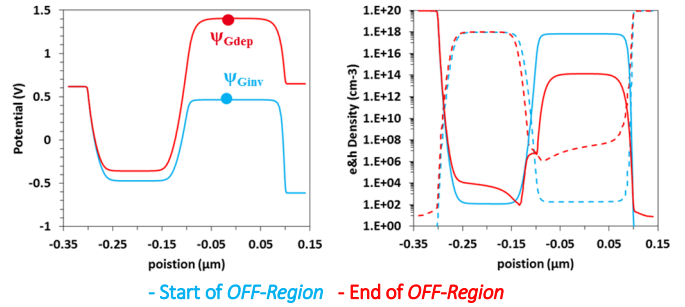
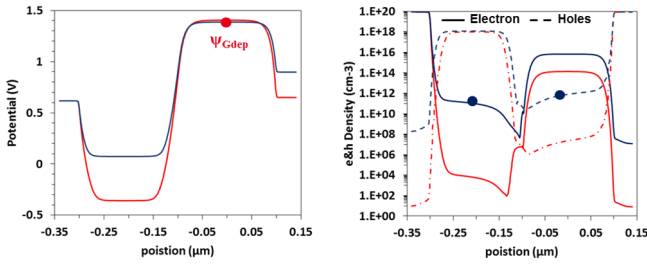


Figure 6: Potential and carrier densities from cathode to anode during *OFF-Region*

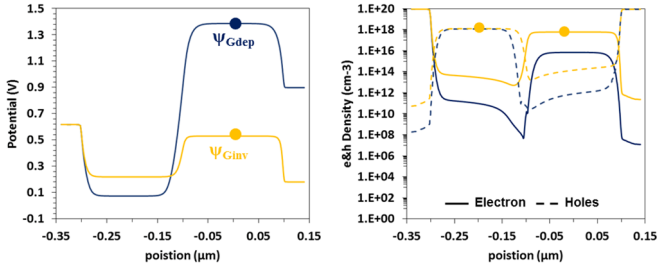
**3-Barriers collapsing:** In this regime, while the anode current increases over 4 decades,  $V_A$  increases from 1.2 to 1.5V. As all electrons under the gate were removed during *OFF-region*, additional increase of  $V_A$  produces the direct polarization of PN junctions. This is evidenced by the product  $n \cdot p > n_i^2$  (Fig.7-a) and it also justifies the strong increase of  $I_A$ . Similarly, increase of  $V_A$  produces an increase of potential in ungated region while potential in gated region stays constant (still equal to its maximum value  $\psi_{Gdep}$ ), leading to a lowering of potential barrier between gated and ungated region (Fig.7-b). Fig.7-a also shows that sharp switch (for  $V_{on}$ , see Fig.2) occurs when electron density in ungated region is equal to hole density in gated region (corresponding to forward polarized PIN diode condition).



- Start of Barriers Collapsing - End of Barriers Collapsing  
 Electron in ungated region = Hole in gated region  
 → sharp switch ( $V_{on}$ )

Figure 7: Potential and carrier densities from cathode to anode during Barriers collapsing

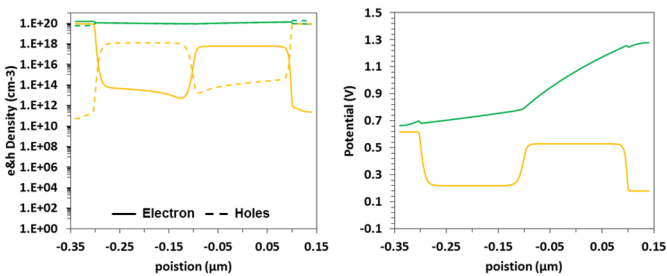
4-Negative resistance:  $V_A$  decreases from 1.5V to 0.8V and  $I_A$  increases by 2 decades. This regime is a kind of transition between the  $Z^2$ -FET off and on states. Electron density increases in the gated region while it reaches hole density value in ungated region (Fig. 8-a). This corresponds to sharp switch ( $V_{off}$  see Fig. 2). The potential in the gated region moves from depletion to inversion values during the negative resistance regime (Fig. 8-b): this provides a usable criterion to evaluate analytically  $V_{off}$ .



- Start of Negative Resistance - End of Negative Resistance  
 Hole in ungated region = Electron in gated region  
 → sharp switch ( $V_{off}$ )

Figure 8: Potential and carrier densities from cathode to anode during Negative Resistance

5-PIN diode:  $Z^2$ -FET acts as a PIN diode forward biased (Fig. 9). Electron and holes concentration are superimposed in this regime, what demonstrates that transport mode has moved from classical MOSFET to ambipolar mode. The full  $Z^2$ -FET DC operation is sketched on Fig. 10.



- Start of PIN diode - End of PIN diode

Figure 9: Potential and carrier densities from cathode to anode during PIN diode mode operation.

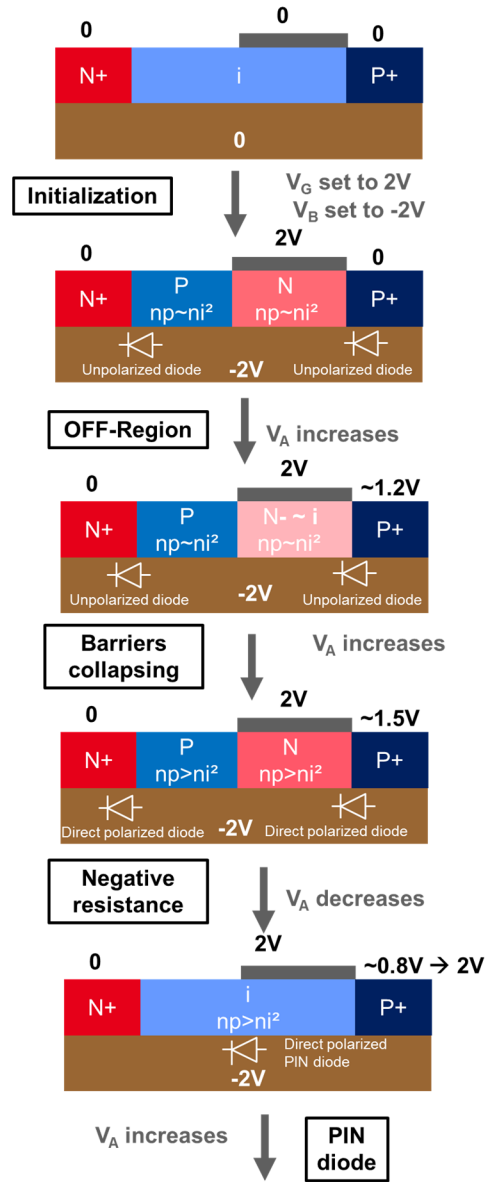


Figure 10: summary of the complete  $Z^2$ -FET DC operation

#### IV. $Z^2$ -FET ANALYTICAL DC MODEL

As  $Z^2$ -FET is a partially gated PIN diode,  $I_A(V_A)$  can be modeled using ref. [7] and considering diode ideality factor of 2, leading to:

$$I_A = I_{La} \left( e^{\frac{V_{APP} - R_{PIN} I_A}{N_{ut}}} - 1 \right) + I_{Rec} \left( e^{\frac{V_{APP} - R_{PIN} I_A}{N_{ut}}} - 1 \right)^2 \quad (1)$$

where  $I_{La}$  and  $I_{Rec}$  respectively stand for diffusion and recombination currents,  $R_{PIN}$  represents the intrinsic region resistance and  $ut = kT/q$ . In PIN diode regime, this equation is used natively ( $V_{APP} = V_A$ ) while in regimes OFF-region and Barriers Collapsing,  $V_{APP}$  has to account for change in potential reference through  $V_{APP} = V_A + \psi_{Ginv} - \psi_G$  (Fig.11).  $\psi_{Ginv}$

(and  $\psi_{Gdep}$ ) are analytically evaluated through an adaptation of Leti-UTSOI model [8].

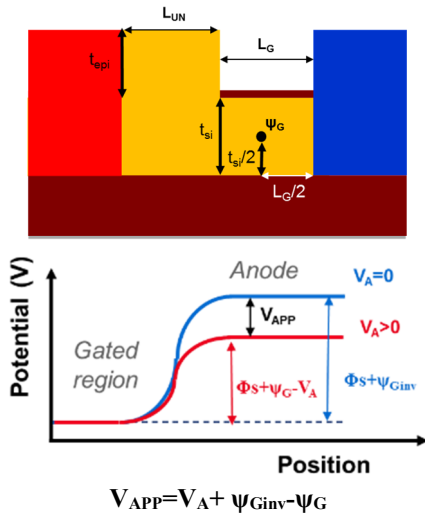


Figure 11: Z<sup>2</sup>-FET modeling parameters and applied voltage  $V_{APP}$  evaluation.

The variations of  $\psi_G$  and  $V_A + \psi_{Ginv}$  are plotted on Fig.12 as a function of  $V_A$ . In *OFF-region*,  $V_{APP}$  is close to zero (dashed green rectangle on Fig.12) and the square term in  $I_A$  can be neglected. As anode current in this regime  $I_{A_{OFF-Region}}$  is weak, the resistance of intrinsic region  $R_{PIN}$  can be neglected. It leads to:

$$I_{A_{OFF-Region}} = I_{La_{OFF-Regime}} \left( e^{\frac{V_{APP}}{N_{ut}}} - 1 \right) \quad (2)$$

In *barriers collapsing* regime,  $V_{APP} \gg R_{PIN} I_A$  (dashed blue rectangle on Fig.12) and the first term of (1) can be neglected and similarly to OFF regime, intrinsic region resistance can be neglected, leading this expression of anode current in *barriers collapsing* regime,  $I_{ABC}$ :

$$I_{ABC} = I_{Rec_{BC}} \left( e^{\frac{V_{APP}}{N_{ut}}} - 1 \right)^2 \quad (3)$$

Since the *negative resistance* region is too complex for physics-based analytical model, we used a behavioral linear dependency of  $I_A$  (in log scale) with  $V_A$  (Fig.2 & 3) linking both switching positions. Fitting our model on TCAD results allowed to reach good accordance as illustrated on Fig. 13.

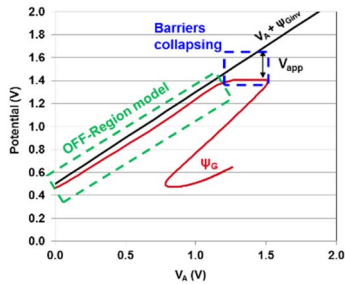


Figure 12: Potential in gated region  $\psi_G$  (red) and  $V_A + \psi_{Ginv}$  as a function of  $V_A$  extracted from TCAD.

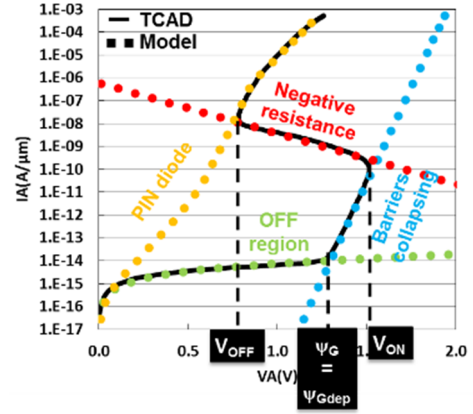


Figure 13: Z<sup>2</sup>-FET analytical models validation by DC TCAD.

## V. CONCLUSION

In this paper, we revealed and explained the complex DC behavior of Z<sup>2</sup>-FET and also proposed an analytical model validated by TCAD simulation. To achieve compact model, analytical evaluation of boundary conditions between each operating regime are necessary ( $\psi_{Gdep}$ ,  $V_{on}$  and  $V_{off}$  shown on Fig.13) together with smoothing functions between each regime to ensure continuity. This model is compatible with the conventional SPICE simulator to finally enable Z<sup>2</sup>-FET circuit simulation and design studies.

## ACKNOWLEDGMENT

The research leading to these results has received funding from the European Union's Horizon 2020 research and innovation program under grant agreement No 687931 REMINDER.

## REFERENCES

- [1] Y. Solaro, J. Wan, P. Fonteneau, C. Fenouillet-Beranger, C. Le Royer, A. Zaslavsky, P. Ferrari, S. Cristoloveanu "Z<sup>2</sup>-FET: A promising FDSOI device for ESD protection," in Solid State Electronics Journal, Vol. 97, July 2014, pp. 23-29.
- [2] J. Wan, S. Cristoloveanu, C. Le Royer, A. Zaslavsky "A feedback Silicon-On-Insulator steep switching device with gate-controlled carrier injection" Solid-State Electronics Journal, Vol. 76, 2012, pp. 109-111
- [3] J. Wan, C. Le Royer, A. Zaslavsky, S. Cristoloveanu "A compact capacitor-less high-speed DRAM using field effect-controlled charge regeneration" in Electron Dev Lett, IEEE, Vol. 33, 2012, pp. 179-181
- [4] H. El Dirani; M. Bawedin; K. Lee; M. Parihar; X. Mescot; P. Fonteneau; Ph. Galy; F. Gamiz; Y-T. Kim; P. Ferrari; S. Cristoloveanu "Competitive 1T-DRAM in 28 nm FDSOI technology for low-power embedded memory" in S3S Tech. Dig. 2016
- [5] Y. Taur, J. Lacord, M. S. Parihar, J. Wan, S. Martinie, K. Lee, M. Bawedin, J.-C. Barbe, S. Cristoloveanu "A comprehensive model on field-effect pnpn devices (Z<sup>2</sup>-FET)" Solid-State Electronics Journal, Vol. 134, 2017, pp. 1-8
- [6] Available: <http://www.synopsys.com>
- [7] E. Gatard PhD dissertation 2006.
- [8] LETI-UTSOI manual, 1.13 May 2012. <http://www-leti.cea.fr/en/How-to-collaborate/Focus-on-Technologies/UTSOI>.